This is the accepted manuscript version of the contribution published as:

Sühnholz, S., Gawel, A., **Kopinke, F.-D.**, **Mackenzie, K.** (2021):
Evidence of heterogeneous degradation of PFOA by activated persulfate – FeS as adsorber and activator
Chem. Eng. J. **423** , art. 130102

The publisher's version is available at:

http://dx.doi.org/10.1016/j.cej.2021.130102

Journal Pre-proofs



Evidence of heterogeneous degradation of PFOA by activated persulfate – FeS as adsorber and activator

Sarah Sühnholz, Alina Gawel, Frank-Dieter Kopinke, Katrin Mackenzie

PII: S1385-8947(21)01687-9
DOI: https://doi.org/10.1016/j.cej.2021.130102
Reference: CEJ 130102

To appear in: *Chemical Engineering Journal*

Received Date: 5 October 2020
Revised Date: 23 April 2021
Accepted Date: 24 April 2021

Please cite this article as: S. Sühnholz, A. Gawel, F-D. Kopinke, K. Mackenzie, Evidence of heterogeneous degradation of PFOA by activated persulfate – FeS as adsorber and activator, *Chemical Engineering Journal* (2021), doi: https://doi.org/10.1016/j.cej.2021.130102

This is a PDF file of an article that has undergone enhancements after acceptance, such as the addition of a cover page and metadata, and formatting for readability, but it is not yet the definitive version of record. This version will undergo additional copyediting, typesetting and review before it is published in its final form, but we are providing this version to give early visibility of the article. Please note that, during the production process, errors may be discovered which could affect the content, and all legal disclaimers that apply to the journal pertain.

© 2021 Elsevier B.V. All rights reserved.

Evidence of heterogeneous degradation of PFOA by activated persulfate – FeS as adsorber and activator

Sarah Sühnholz[a], Alina Gawel[b], Frank-Dieter Kopinke[a] and Katrin Mackenzie[a]*

[a] Helmholtz Centre for Environmental Research - UFZ, Department of Environmental Engineering, Permoserstr. 15, D-04318 Leipzig, Germany

[b]Fraunhofer Institute for Environmental, Safety, and Energy Technology UMSICHT, Division Energy, Osterfelder Straße 3, D-46047 Oberhausen, Germany

***Corresponding Author**

Email: sarah.suehnholz@ufz.de. Phone: +493412351584

Journal Pre-proofs

Abstract

Perfluorinated alkyl acids, such as perfluorooctanoic acid (PFOA), are extremely persistent water contaminants. Persulfate activation has already been described as a possible strategy for oxidizing PFOA, although the reaction of sulfate radicals with PFOA is challenging in the presence of common water constituents such as inorganic ions and natural organic matter, which strongly compete for sulfate radicals. The present study investigated FeS-assisted heterogeneous activation of persulfate for degradation of PFOA in water matrices. This approach breaks the dominance of the bulk-phase competitors for sulfate radicals, thus PFOA is also degraded in the presence of natural organic matter (up to 100 mg L^{-1}), Cl^- and NO_3^- (up to 100 mM). The hypothesis of heterogeneous reaction is supported by kinetic isotope effect measurements and a change in product pattern, and therefore a shift in participation of the various reaction pathways compared to homogeneous PFOA degradation. Significant PFOA degradation was achieved at moderate PFOA concentrations ($c_{0,PFOA}$ = 1 mg L^{-1}) over a broad range of reaction conditions, although it is most efficient at higher reactant concentrations.

PFOA enrichment at the FeS surface is higher (K_D = 100 – 500 L kg^{-1}) than expected for a mineral with almost no inner surface; it seems to be the pre-requisite for reactions of radical consumers near the FeS surface and in the water matrix to be partially decoupled from each other.

KEYWORDS: Perfluorooctanoic acid; heterogeneous; persulfate activation; iron sulfide; surface enrichment

1 Introduction

In recent decades, per- and polyfluorinated alkyl substances (PFAS) have become a topic of high relevance in environmental literature [1-5]. PFAS are on the one hand hydrophobic due to a long fluorinated alkyl chain, but on the other hand they often show surfactant-like properties when hydrophilic functional end groups are present. In contrast to conventional surfactants, PFAS are reported as lipophobic but still were found to bioaccumulate. They are widely used in industrial, commercial, and consumer applications, e.g. in polymer production, fire retardants, aqueous film forming foams (AFFF), and oil- and water-repellent coatings. Due to this multitude of applications as well as their high chemical persistence and bioresistance, PFAS have been determined worldwide in inland waters at up to μg L^{-1} concentrations [4]. Most of the attention has been given to perfluorooctane sulfonate (PFOS) or perfluorooctanoic acid (PFOA), on which recent regulatory measures were mainly focused [6]. In 2009, PFOA and PFOS were included as persistent organic pollutants in the Stockholm Convention. They are found in groundwater bodies all over the world. Especially in the proximity of sites where PFAS-containing AFFF were used for firefighting, the concentrations in groundwater can reach the mg L^{-1} range [7, 8]. Therefore, novel *in-situ* remediation technologies are highly desirable in order to avoid long-term application of measures such as pump-and-treat for protecting drinking-water catchment areas [9, 10]. In the literature, numerous approaches for PFOA and PFOS removal from aqueous media are described, which can be separated into two groups: adsorptive extraction and chemical degradation methods [11]. Some examples for the latter strategy are sonolysis [12], electrochemical treatment [11, 13, 14], photooxidation/photocatalysis [15-19], oxidation with sulfate radicals [20, 21] and reduction with zero-valent iron in subcritical water [22].

However, most of these degradation approaches are not applicable to groundwater conditions. In addition, some of the mentioned advanced oxidation processes (AOPs) are limited to degrading

perfluorinated carboxylic acids. The reaction mechanism is electron transfer from the anionic PFAS head group to the oxidant, leading to gradual breakdown of these substances after reaction with the head group [22, 23]. Hydroxyl radicals are not capable of performing such reactions, but sulfate radicals are [24, 25]. For perfluorinated sulfonic acids with lower electron density at the head group, the literature provides contradictory information about the ability of sulfate radicals to degrade them [23, 26]. Our own results lead to the conclusion that these compounds are not degradable with sulfate radicals. However, the sulfonic acids are a problem of the past because perfluorinated compounds have been replaced by polyfluorinated substitutes. These can be biodegraded and perfluorinated carboxylic acids are usually formed. PFOA, as the most studied perfluorinated carboxylic acid (and also the one with the regulatory requirements), was chosen in this study to represent the class of perfluorinated carboxylic acids [27].

Sulfate radicals can be generated by activation of peroxydisulfate (PS, $S_2O_8^{2-}$), and have already been applied for the degradation of persistent pollutants in water [28]. The most effective and common activation methods for PS are UV radiation and enhanced temperature [29]. Additionally, PS activation based on microwave irradiation and the presence of transition metals or carbon materials has been reported [29-32]. Therefore, environmentally compatible iron species, such as zero-valent iron, dissolved Fe^{2+} and iron minerals, are worthy of attention for PS activation. The reactions with iron metal and ferrous iron proceed according to eqs. 1 and 2 [29, 33]:

$$Fe^0 + 2\ S_2O_8^{2-} \rightarrow Fe^{2+} + 2\ SO_4^{\bullet-} + 2\ SO_4^{2-} \quad (1)$$

$$Fe^{2+} + S_2O_8^{2-} \rightarrow Fe^{3+} + SO_4^{\bullet-} + SO_4^{2-} \quad (2)$$

However, there are two significant disadvantages of persulfate activation driven by dissolved Fe^{2+}: i) half of the persulfate oxidation capacity is consumed in the activation step, and ii) the ability of Fe^{2+} to quench the generated sulfate radicals with a high rate constant (k_3) results in further losses

according to eq. 3. Therefore, Fe^{2+} can become a serious competitor to any (especially slow reacting) pollutant to be degraded [34].

$$Fe^{2+} + SO_4^{\bullet-} \rightarrow Fe^{3+} + SO_4^{2-} \qquad k_3 = 9.9 \cdot 10^8\ M^{-1}\ s^{-1}\ [35] \qquad (3)$$

Recent studies report that FeS, due to its poor water solubility, can be used as a slow-releasing source of dissolved Fe^{2+} in low concentrations [34, 36-39]. Thereby, the assumption is made that sulfate radical formation takes place exclusively by homogenous reaction according to eq. (2) [34, 36, 39]. However, in recent publications about FeS as PS activator, a heterogeneous activation reaction with radical formation at the FeS surface and subsequent radical diffusion into the liquid phase is discussed [37]. Thereby, catalytic activation of PS by surface-assisted homolytic bond cleavage yielding two sulfate radicals is conceivable [40]. This means that activation with FeS as catalyst has clear advantages over activation with dissolved iron, and offers in addition lower treatment costs due to a catalytic activator and therefore higher radical yields. If PFOA is to be degraded in natural and not in pure water, radical quenchers such as nitrate, carbonate, chloride and organic matter, which all react faster with sulfate radicals than PFOA ($k_{SO4-\bullet+PFOA} = 1.6 \cdot 10^4$ $M^{-1}\ s^{-1}$ [41]), have to be considered (see eqs. 4-6) [35, 42, 43].

$$NO_3^- + SO_4^{\bullet-} \rightarrow NO_3^{\bullet} + SO_4^{2-} \qquad k_4 = 10^5 - 10^6\ M^{-1}\ s^{-1}\ [35] \qquad (4)$$

$$CO_3^{2-} + SO_4^{\bullet-} \rightarrow CO_3^{\bullet-} + SO_4^{2-} \qquad k_5 = 4.1 \cdot 10^6\ M^{-1}\ s^{-1}\ [43] \qquad (5)$$

$$Cl^- + SO_4^{\bullet-} \rightarrow Cl^{\bullet} + SO_4^{2-} \qquad k_6 = 10^8\ M^{-1}\ s^{-1}\ [35] \qquad (6)$$

The adsorptive enrichment of PFOA on the FeS surface may compensate for its lower reactivity towards sulfate radicals compared to the matrix components and offers a spatial separation of PFOA enriched in the reaction zone (activator surface) and the more reactive competitors dissolved in the water matrix. Therefore, application of crystalline FeS as activator offers two advantages: i)

FeS releases only low concentrations of Fe^{2+} with a low dissolution rate, and ii) sulfate radicals arise at the surface in direct proximity to the adsorbed PFOA.

Based on the increasing demand for remediation approaches for PFOA-contaminated sites, a great potential of FeS for PS activation for oxidative water purification can be derived. For this reason, the oxidation system PS + FeS was examined for PFOA degradation under various conditions. The aim of the present study is to demonstrate the feasibility that PFOA can be degraded using an iron mineral, despite the fact that dissolved iron(II) (omnipresent since the mineral dissolves) reacts faster with sulfate radicals than with PFOA. This is seen as a big step forward and has not previously been achieved. Another major aspect is to show the degradation capability of the FeS + PS system with regard to PFOA in natural groundwater samples and in the presence of site sediment.

2 Materials and methods

2.1 Sorption experiments

In order to determine the adsorption behavior of PFOA on crystalline FeS particles (Fluka, technical grade, d_{50} = 20 µm, specific surface area SSA_{BET} = 0.9 $m^2\ g^{-1}$ measured by us, XRD Fig. S1 in SI section), a particle concentration of 500 mg L^{-1} (5.7 mM) and PFOA (Sigma-Aldrich, 96%) concentrations between 0.1 and 20 mg L^{-1} ($2.4 \cdot 10^{-4}$ – $4.8 \cdot 10^{-2}$ mM) were adjusted in 30 mL PE-vials at pH = 7 and at pH = 3. The samples were equilibrated for one week at room temperature by continuous shaking. Subsequently, 1 mL of the suspension was filtered with a 0.2 µm syringe filter (cellulose acetate membrane, Sartorius) and the freely dissolved concentration of PFOA was measured with HPLC-MS (Shimadzu LC-MS2020 with Phenomenex Gemini® 3 µm C_6-Phenyl 110 Å, LC Column 100 x 2 mm). Afterwards the vials were centrifuged, the supernatant discarded

and the particles extracted with methanol (Sulpelco, HPLC grade). The extracted PFOA was measured with HPLC-MS in negative scan and SIM mode (m/z = 413, 363, 313, 263, 213 amu for PFOA and shorter chain acids, LOD = 0.03 µg L^{-1} and LOQ = 0.06 µg L^{-1}). The extraction recovery was between 70 and 90 %, leading to an overall recovery (adsorbed + dissolved fraction) of around 95 %. The variation of the peak areas in the repeated measurement of one sample is < 1 % and for repeated experiments is on average 3.5 %.

2.2 Degradation experiments

All experiments were carried out at room temperature (22 ± 2°C) and at least as duplicates. The resulting error bars in the figures represents the deviation from the mean value.

2.2.1 Influence of the reaction conditions on PFOA degradation

In order to find optimal reaction conditions, PFOA degradation in matrix-free, deionized water was performed, varying either initial PS, FeS or PFOA concentrations in 60 mL glass vials (Table 1). Glass vials were used instead of PE-vials in order to minimize side reactions of sulfate radicals with the reactor wall.

Table 1: Initial concentrations of PFOA, FeS, and PS in degradation experiments in 40 mL deionized water.

Variable compound	$c_{0,PFOA}$ **[mg L^{-1}]**	$c_{0,PFOA}$ **[mM]**	$c_{0,PS}$ **[g L^{-1}]**	$c_{0,PS}$ **[mM]**	c_{FeS} **[mg L^{-1}]**	c_{FeS} **[mM]**
PFOA	1 to 2800	$2.4 \cdot 10^{-3}$ to 6.7	30	126	40	0.45
PS	2800	6.7	2 to 30	8.4 to 126	40	0.45
FeS	2800	6.7	30	126	40 to 1000	0.45 to 11.4

Before starting the degradation experiments by PS addition, the aqueous suspensions were inspected for their blank fluoride and free PFOA concentrations after reaching the sorption equilibrium at the FeS particles. Fluoride was analyzed by means of ion chromatography (Dionex IC DX 500, equipped with IonPac AS11-HC column, 4 x 250 mm; LOD = 0.05 mg L^{-1} and LOQ = 0.1 mg L^{-1}) or an ion-selective electrode (F 800 DIN, WTW, Weilheim, Germany; LOD = 0.01 mg L^{-1} and LOQ = 0.1 mg L^{-1}), PFOA and shorter-chain PFAS (PFHA = Perfluoroheptanoic acid, PFHxA = Perfluorohexanoic acid, PFPA = Perfluoropentanoic acid, PFBA = Perfluorobutanoic acid) by HPLC-MS. PS ($Na_2S_2O_8$, Carl Roth, >99%) addition to the solutions marks the reaction start (t_0). Over the reaction duration of one week, light was excluded by carefully covering the glass reactor with black cloth. Aliquots of 1 mL were frequently taken, filtered with 0.2 µm syringe filters and analyzed for their fluoride and PFOA concentrations as well as for shorter-chain perfluorinated acids as expected degradation products.

2.2.2 Influence of the matrix compounds on PFOA degradation

The influence of specific compounds typically occurring in groundwater on the degradation of PFOA was examined with FeS-activated PS in 60 mL glass vials. PFOA ($c_{0,PFOA}$ = 10 mg L^{-1}) degradation was performed in the presence of NOM ($c_{0,NOM}$ = 1 to 100 mg L^{-1}; Suwannee River natural organic matter (NOM), reference number: 2R101N [44]), Cl^- (NaCl, Merck, p.a.) and NO_3^- ($NaNO_3$, Riedel-de-Haën, p.a.) ($c_{0,Cl-/NO3-}$ = 1 to 100 mM) with FeS ($c_{0,FeS}$ = 0.5 g L^{-1}) as PS activator at a starting pH = 7 in 40 mL water. PS ($c_{0,PS}$ = 30 g L^{-1}) was added to the suspensions to start the reaction. The suspensions were allowed to react for one week under light exclusion. Analyses were carried out as described in 2.2.1.

2.2.3 Fate of perfluoroalkyl radicals in FeS-activated suspensions vs. homogeneous solutions

We conducted a number of experiments with PFOA (c_0 = 0.25 mM) + PS (c_0 = 100 mM) in aqueous solution (100 mL, t = 240 h, pH_0 = 5 to 2) and in FeS suspension (t = 24 h, c_{FeS} = 500 mg L^{-1}) at ambient temperature. The reaction mixtures were initially purged with Ar to remove dissolved O_2. The headspace phase above the aqueous reaction mixtures (1:10 v/v) was sampled with a gas syringe (250 µL) and analyzed by means of GC-MS.

2.2.4 Influence of natural water matrices and sediment on PFOA degradation

The experiments were conducted in 100 mL glass vials using various water matrices (50 mL deionized water, tap water or groundwater from a PFAS-contaminated site in North Rhine-Westphalia, Germany) with or without addition of 100 g L^{-1} site sediment with a starting pH = 7. The PFOA concentration of each sample, including the groundwater samples, was adjusted to $c_{0,PFOA}$ = 10 mg L^{-1}. FeS was added at a concentration of $c_{0,FeS}$ = 1 g L^{-1}, PS of $c_{0,PS}$ = 30 g L^{-1}. Before adding PS, the samples were allowed to reach sorption equilibria with the mineral surface and the sediment, whereby the sediment does not reduce the PFOA concentration significantly. Sampling and analyses were carried out as described in 2.2.1.

3 Results and discussion

3.1 Sorption of PFOA on FeS surface

In Figure 1, the sorption isotherms of PFOA on FeS at pH 3 and pH 7 are plotted. The adsorption follows a type V isotherm, meaning that only moderate loadings can be achieved at low adsorptive concentrations. At higher adsorptive concentration, loading increases due to the promotion of further adsorption by the presence of the adsorbate [45]. This isotherm curve is characteristic for the adsorption of polar compounds on hydrophobic surfaces.

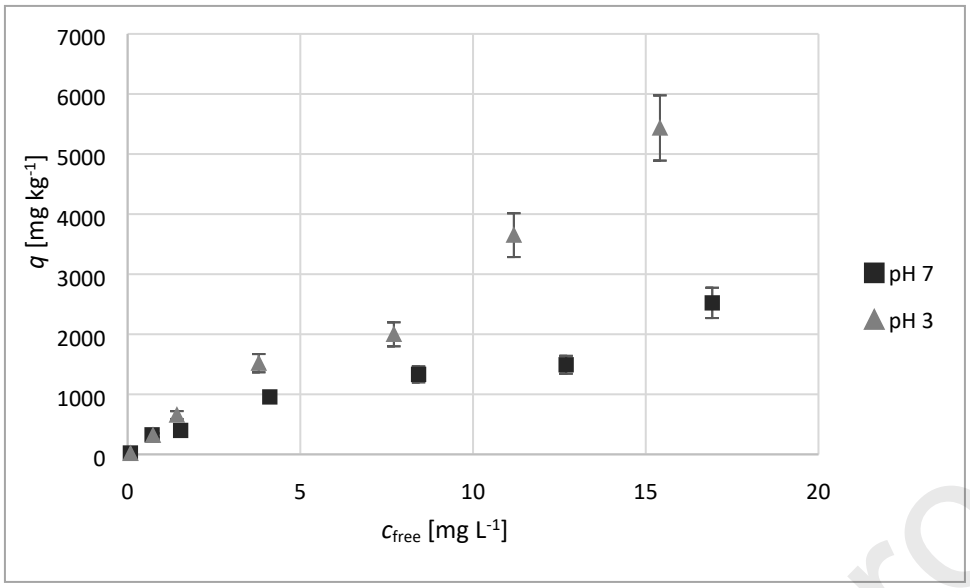


Figure 1: Adsorption isotherm of PFOA on FeS ($c_{particle}$ = 0.5 g L^{-1} = 5.7 mM, pH = 3 or 7, $c_{0,PFOA}$ = 0.1-20 mg L^{-1} = 2.4 · 10^{-4} – 4.8 · 10^{-2} mM). FeS loadings (q) were confirmed by extraction of FeS with methanol. Error bars represent deviations of single values from the mean value of at least two independent measurements.

At high PFOA concentrations, the loading on the FeS surface is much higher than expected for a material with almost no inner surface. More than 0.5 wt-% loading could be reached, whereas for other minerals a maximum loading of 0.1 wt-% was reported [46]; compared to other iron minerals, the loading is five to eight times higher for FeS at c_{PFOA} = 10 mg L^{-1} = 4.8 · 10^{-2} mM and $c_{iron\ mineral}$ = 0.5 g L^{-1} = 5.7 mM at pH 7 (refer to Figure S3). Furthermore, K_D values between 100 and 300 L kg^{-1} at pH 7 were calculated, again remarkably high with regard to the small specific surface area (0.9 m^2 g^{-1}). Even higher are the K_D values at pH 3 (up to 500 L kg^{-1}), where FeS receives a positive surface charge and electrostatic attraction plays a supporting role [47]. Furthermore, the geometric surface area of 20 µm FeS spheres is only approximately 0.06 m^2 g^{-1}. Hence, the measured surface area of 0.9 m^2 g^{-1} may result from the surface roughness or a low but significant porosity of the FeS. 0.5 wt-% PFOA loading corresponds to a mean sorbate layer thickness of about 6 nm. This would correspond to approximately 6 PFOA layers if one assumes a micellar arrangement of the chains and a molecular size of 13.6 x 6.5 $Å^2$ [48]. A typical surfactant bilayer

micelle should contain 2 layers. As an alternative to the formation of surface layers, one could assume the filling of the existing pores. In conclusion, although FeS is only a slightly porous material, a trap-and-degrade approach seems possible, especially at lower pH values.

3.2 Influence of the reaction conditions on PFOA degradation in pure water

Figure 2 summarizes the results of the PFOA oxidation experiments with FeS-activated PS after 7 d reaction time under variation of reactant starting concentrations. In batches with varying PS and FeS concentrations, high PFOA concentrations ($c_{0,PFOA} = 2.8$ g L^{-1}) were chosen in order to obtain measurable PFOA degradation and thereby fluoride formation in the presence of reactive quenchers (i.e. $c_{0,PFOA} \cdot k_{SO4-\bullet+PFOA} \geq c_{0,quencher} \cdot k_{SO4-\bullet+quencher}$). We are aware that these concentrations are not environmentally relevant; they were only used to determine the feasibility of PFOA degradation with FeS-activated PS. We wanted to learn about the system and its functional principle, and subsequently to share the knowledge gained for further optimization as well as for transferability to lower PFOA concentration levels.

The fluoride yield was normalized to complete mineralization of PFOA to F^- and CO_2. Product yields less than 100 % are due to gaps in the balance sheet, which will be discussed later.

Journal Pre-proofs

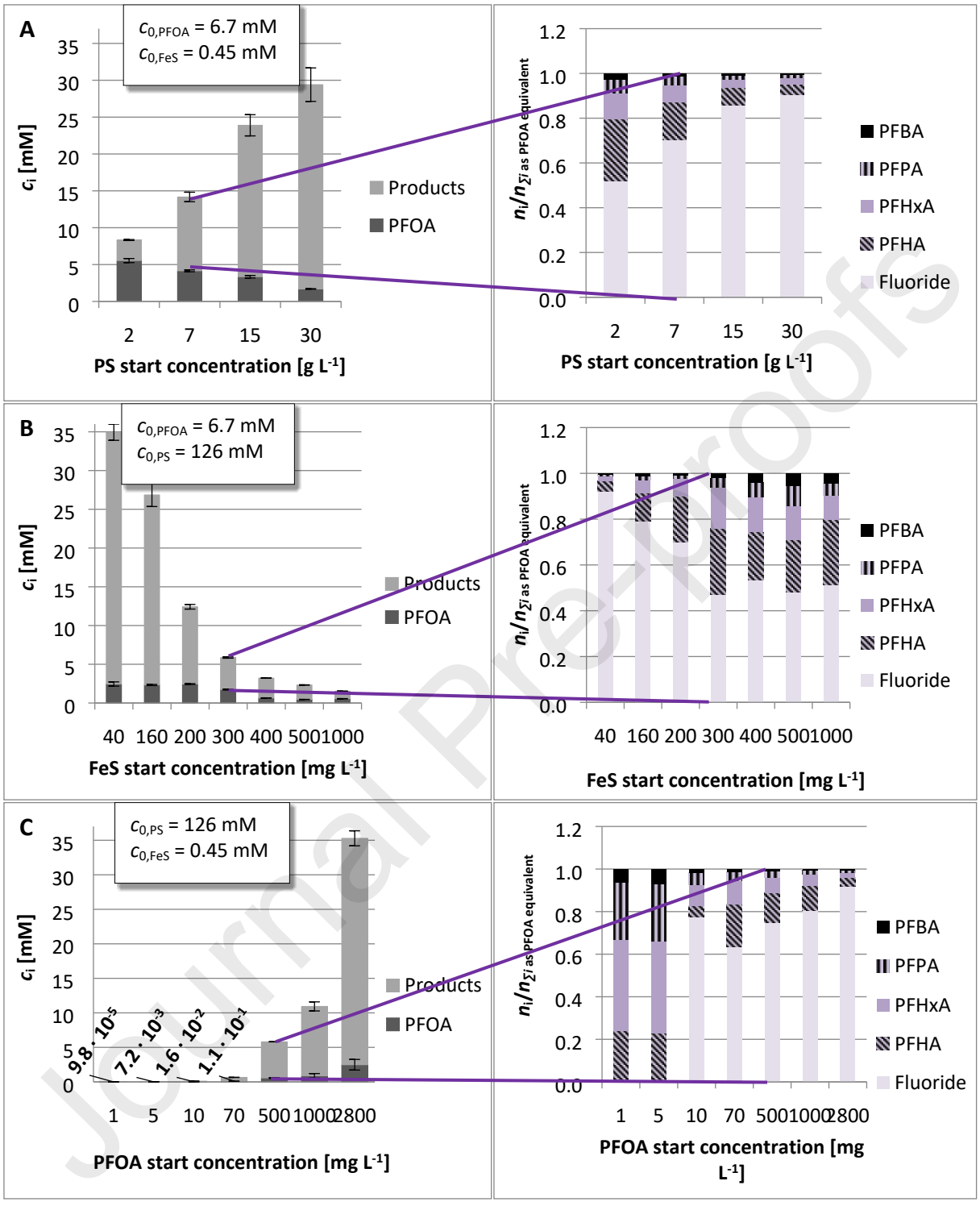


Figure 2: Influence of PS (A), FeS (B) and PFOA (C) starting concentrations on the PFOA conversion degrees and molar product yields with FeS-activated persulfate after 7 d of reaction time. Left: residual PFOA and product concentrations (fluoride yield referenced to complete PFOA mineralization) and right: product

distribution related to sum of PFOA equivalents (*n* is the mole number); $pH_{start} \leq 7$, $pH_{final} \leq 2$. Error bars represent deviations of single values from the mean value of at least three independent experiments.

When pH was not controlled it fell to pH ≤ 2 due to fast PS activation during the reaction. Under these strongly acidic conditions, FeS dissolves slowly over time (about 60 % after 7 d, compare with Figure S7); both iron and the sulfide are oxidized under these conditions to Fe(III) and sulfate/sulfite [37, 40]. Favored PFOA degradation at low pH values has already been described in other studies [49-51]. One possible explanation is the protonation of sulfate radicals ($pK_a \approx 0$), leading to a higher reactivity [52]. If these neutral radicals ($HSO_4^{\bullet}$) were very reactive towards PFOA, they could dominate the PFOA degradation kinetics despite their small proportion. Furthermore, at pH < 3, a positive surface charge of FeS (isoelectric point $pH_{i.e.p.} = 3.3$) occurs, leading to a higher sorption affinity due to preferred electrostatic interactions between FeS and PFOA [47]. Our own adsorption data confirm this (Figure 1).

In Figure 2A, the influence of PS concentration on PFOA degradation is illustrated. As might be expected, the reaction is faster at higher PS concentrations. For the chosen PFOA concentration, PS concentrations below 2 g L^{-1} did not give rise to significant fluoride release. This indicates the requirement for a certain minimum concentration of PS in order to ensure an oxidation strength sufficient to overcome the competing quenching reactions [21]. Since the highest PFOA conversion and fluoride yield were found at a PS concentration of 30 g L^{-1}, this concentration was chosen for subsequent experiments.

Figure 2B shows the results of oxidative PFOA degradation at various FeS concentrations. Both fluoride yields and PFOA concentrations decrease with increasing FeS concentrations after the 7 d reaction time. In the case of PFOA, this observation is to be expected, as higher activator concentrations lead to higher sulfate-radical concentrations. Thereby, higher degradation rates and degrees are reached. Shorter-chain products from perfluoroheptanoic acid (PFHA) to

Journal Pre-proofs

perfluorobutanoic acid (PFBA) were quantified by means of HPLC-MS. However, the corresponding fluoride concentrations were not detected: instead, a large balance gap was observed. We assign the missing fluoride partly to reaction with the glass wall of the reaction vials according to eq. 7 [53].

$$SiO_2(s) + 6\ HF(aq) \rightarrow 2\ H_2O + H_2SiF_6(aq) \quad (7)$$

The balance gap resulting from the wall reaction depends on the pH value and is approximately 85% at a pH ≈ 1 (compare SI part).

It is furthermore conceivable that fluoride species adsorb to the FeS surface. Chemisorption of fluoride to iron-containing materials has been reported [54]. The adsorption affinity was found to increase with decreasing pH, because surface charge becomes more positive, leading to electrostatic interactions. It has been stated that this kind of adsorption is largely irreversible [54]. In order to confirm this hypothesis, a suspension of FeS (2.5 g L^{-1}) in fluoride solution (5 mg L^{-1}) was equilibrated at pH ≈ 1 (adjusted with sulfuric acid) in polyethylene vials for one week in order to determine fluoride recovery (see Table S4). Only 84% of the initial fluoride concentration was retrieved. Addition of 2.5 g L^{-1} PS decreased the fluoride recovery to 60%. The latter phenomenon of decreased fluoride recovery caused by addition of oxidizing agents in the presence of iron sulfides is known from the literature [55]. In summary, the growing balance gap with increasing FeS concentrations is most probably related to the more complete mineralization of PFOA accompanied by fluoride losses, as higher FeS concentrations lead to more fluoride bound to the surface. This reduces the measurable fluoride concentration although more fluoride was produced.

Figure 2C confirms that considerable degradation of PFOA occurred for all initial PFOA concentrations (minimum 35 % degradation). Formation of shorter-chain products was observed to a marked degree, even at the lowest applied PFOA concentration of 1 mg L^{-1} (10 % shorter-

chain products). For the experiments with $c_{PFOA,0} \leq 5$ mg L^{-1}, one has to bear in mind that fluoride analysis is less reliable due to the high background concentration of ions (e.g. sodium sulfate) and the relatively low maximum fluoride concentrations (for $c_{PFOA,0} = 5$ mg L^{-1} $c_{F-,max} = 3.5$ mg L^{-1}). At higher PFOA starting concentrations ($c_{0,PFOA} > 70$ mg L^{-1}), turnover (in mol s^{-1}) of PFOA is increased due to its statistical advantage. However, at starting concentrations of PFOA below 10 mg L^{-1}, the removal of PFOA is also increased. In these cases, a higher proportion of PFOA is present in the adsorbed state at the FeS surface, possibly giving rise to sorption-assisted transformations. This means that the concentration ratios between PFOA and radical quenchers on the FeS surface (radical generation site) are different from those in the bulk phase; this changes the probability of the reaction of sulfate radicals in favor of PFOA attack. The larger gap in the mass balance at higher PFOA starting concentrations remains as an unresolved issue. Lutze *et al.* (2017) also observed an open mass balance and suspected the formation of undetected perfluorinated peroxides from perfluoroalkoxy radicals [21]. Furthermore, recent studies have shown that at high concentrations of PFOA, cross-linked fluorinated chains are formed during degradation with sulfate radicals [56]. To a smaller extent, volatile compounds such as perfluorinated alkanes and 1H-perfluoroalkanes are also formed, as discussed in section 3.4.

To summarize: the remaining gap in the mass balances observed in most experiments can be attributed, on the one hand, to the formation of C_2- and C_3-short-chain perfluorinated acids, volatile compounds and possibly also perfluorinated peroxides as well as cross-linked fluorinated chains, none of which were detectable by HPLC-MS analysis. On the other hand, adsorption of PFOA and its degradation products to FeS also leads to a gap in the mass balance. However, with decreasing chain length the extent of adsorption to FeS decreases. Additionally, fluoride was also found to adsorb to FeS (see Table S4) to a considerable extent. This leads to a systematic underestimation of fluoride formation.

Altogether it could be shown that the system FeS/PS is able to degrade PFOA in aqueous suspensions. Although the parasitic radical consumption by dissolved iron is low in FeS-based systems, other radical consumers, which are typically present in groundwater, have to be tested for their inhibitory effects.

3.3 Influence of the water constituents on PFOA degradation by FeS-activated PS

Table 2 illustrates that the reaction of PFOA with sulfate radicals has only a low degree of statistical probability in the presence of typical groundwater constituents. Especially when considering the typically occurring concentration ranges of these matrix compounds, their relative reaction rates with sulfate radicals are several orders of magnitude higher than that of PFOA ($r_i/r_{PFOA} = 10^2$ to 10^8, see Table 2). Hence, no measurable PFOA degradation should be expected in homogeneous solution.

Based on the findings of the experiments shown in Figure 2, it was decided to use 30 g L^{-1} persulfate for the subsequent experiments. Although PFOA is also degraded at lower concentrations of PS, a higher PS concentration leads to a higher degradation rate and clearer differences between the matrix effects become apparent. The negative aspect of this is that the pH value drops sharply and that this can also influence the reaction (see discussion in 3.2). However, since pH has no significant influence on the degree of protonation of the investigated anions added as possible competitors for sulfate radicals (all very weak bases), pH should not interfere with the comparison of the reactions with and without salt addition. For NOM, this is discussed separately. Another aspect of the high PS concentration is that it can cause the PS itself to act as a sulfate radical quencher. This could lead to the assumption that the influence of the other quenchers is low. However, Table 2 shows that at the concentrations applied, the main quenchers are chloride, NOM and dissolved iron. Only the relative reaction rate of nitrate is lower than that of PS. Since the

Journal Pre-proofs

concentration of PS decreases over time, the influence of nitrate over the reaction time becomes greater and can therefore be discussed.

Our experimental results are illustrated in Figure 3. Remarkably, significant PFOA conversion was observed in most degradation experiments regardless of the applied radical quencher, although the reaction of sulfate radicals is much faster with all other water constituents, including water itself and PS (see Table 2), even at relatively high PFOA concentrations (10 mg L^{-1}). The non-environmentally relevant PFOA concentrations were chosen in order to observe reliable results for fluoride formation and shorter-chain intermediates in order unambiguously to prove PFOA oxidation rather than only its 'disappearance'. Neither NOM nor nitrate had significant influence on PFOA degradation by FeS-activated PS. In the case of nitrate, this observation has already been made in another study [20]. For NOM, strong quenching effects were expected as reported for other easily oxidizable substances in tests with heat-activated PS [57, 58]. A fraction of the humic acid precipitates under acidic conditions, thus is withdrawn from the solution phase and therefore to a large extent from direct attack by the short-lived radicals in the bulk phase [59]. In addition, NOM slightly decreases the adsorption of PFOA on the FeS surface (see Figure S4). Despite all these factors, increasing NOM concentrations would be expected to effect a decrease in PFOA degradation. However, this was not observed.

Journal Pre-proofs

Table 2: Estimation of relative reaction rates of various water constituents with sulfate radicals.

	Solute concentration c_0 [M]	**Rate constant with sulfate radicals k [M^{-1} s^{-1}]**	**$c_{solute} \cdot k$ [s^{-1}]**	**Relative rates r_{solute}/r_{PFOA} [-]**	**Ref.**
PFOA	$2.4 \cdot 10^{-5}$	$1.6 \cdot 10^{4}$	0.4	1	[41]
Chloride	$1 \cdot 10^{-3}$ $1 \cdot 10^{-2}$ 0.1	$(2.5…5) \cdot 10^{8}$	$2.5…5 \cdot 10^{5}$ $2.5…5 \cdot 10^{6}$ $2.5…5 \cdot 10^{7}$	$\approx 10^{6}$ $\approx 10^{7}$ $\approx 10^{8}$	[60]
Hydroxide pH = 8	$1 \cdot 10^{-6}$	$1.4 \cdot 10^{7}$	14	≈ 10	[61]
Nitrate	$2 \cdot 10^{-3}$ $2 \cdot 10^{-2}$ 0.2	$3 \cdot 10^{4}$	30 $3 \cdot 10^{2}$ $3 \cdot 10^{3}$	$\approx 10^{2}$ $\approx 10^{3}$ $\approx 10^{4}$	[62]
$Iron(II)_{dissolved,max}$ $Iron(II)_{dissolved,min}$	$\approx 1.1 \cdot 10^{-2}$ $\approx 3.6 \cdot 10^{-4}$	$9.9 \cdot 10^{8}$	$1.1 \cdot 10^{7}$ $3.6 \cdot 10^{5}$	$\approx 10^{7}$ $\approx 10^{6}$	[35]
Water	55.56	60	$3.3 \cdot 10^{3}$	$\approx 10^{4}$	[35]
PS	0.126	$1.2 \cdot 10^{6}$	$1.5 \cdot 10^{5}$	$\approx 10^{5}$	[35]
NOM [(1)]	0.5 5 50	$6.8 \cdot 10^{3}$	$3.4 \cdot 10^{3}$ $3.4 \cdot 10^{4}$ $3.4 \cdot 10^{5}$	$\approx 10^{4}$ $\approx 10^{5}$ $\approx 10^{6}$	[63]

[(1)] concentration in mgC L^{-1} and rate constant in L mgC^{-1} s^{-1}

Journal Pre-proofs

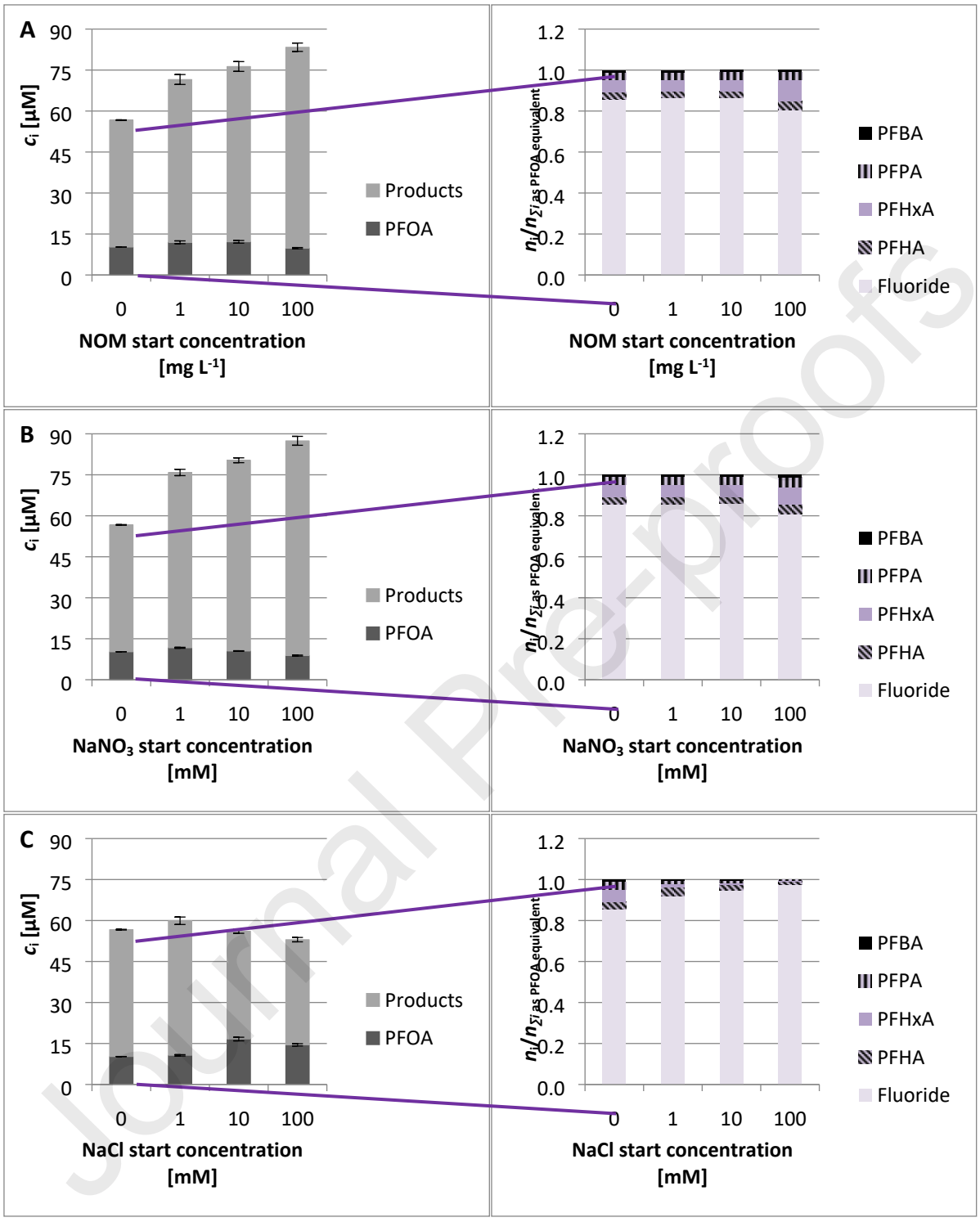


Figure 3: Influence of NOM (A), $NaNO_3$ (B) and NaCl (C) starting concentrations on the PFOA conversion degrees with FeS-activated persulfate after 7 d of reaction time. Left: residual PFOA and product concentrations (fluoride yield normalized to complete PFOA mineralization) and right: product distribution related to sum of PFOA equivalents (*n* is the mole number); $c_{0,PFOA}$ = 10 mg L^{-1} = 2.4 · 10^{-2} mM, $c_{0,PS}$ = 30 g L^{-1}

= 126 mM, $c_{0,FeS}$ = 0.5 g L^{-1} = 5.7 mM, pH_{start} = 7, $pH_{final} \leq 2$. Error bars represent deviations of single values from the mean value of at least two independent experiments.

The oxidation of PFOA by sulfate radicals in the presence of even high chloride concentrations (up to 100 mM) is striking. Such high concentrations are comparable to seawater or chloride-contaminated wastewater, and are usually considered as a key reason why sulfate-radical-based treatment options do not apply for these systems [21]. It has already been reported in the literature that low chloride concentrations have no major adverse influence on PFOA degradation by sulfate radicals. At chloride concentrations higher than 10 mM, the degradation rate drops significantly, accompanied by the preceding oxidation of Cl^- to ClO_3^- or HOCl resulting in OH-radicals [49, 64] (a detailed reaction scheme is provided in the SI). From Figure 3C, a slight decrease in PFOA degradation for higher chloride concentrations can be seen, thus a decrease in degradation rate can also be confirmed in the present study. However, the extent of rate reduction is lower than reported in previous studies (factor 2 rather than factor 3 to 10) [20, 49, 51]. It is remarkable that the fraction of short chain acids as intermediates of the PFOA degradation decreases with increasing chloride concentration by about one order of magnitude, while fluoride generation seems unaffected. This points to a variation in the degradation mechanism and a possible participation of chlorine radicals (or derived species, such as $Cl_2^{-\cdot}$). Since this was not within the scope of this study, further investigations are needed.

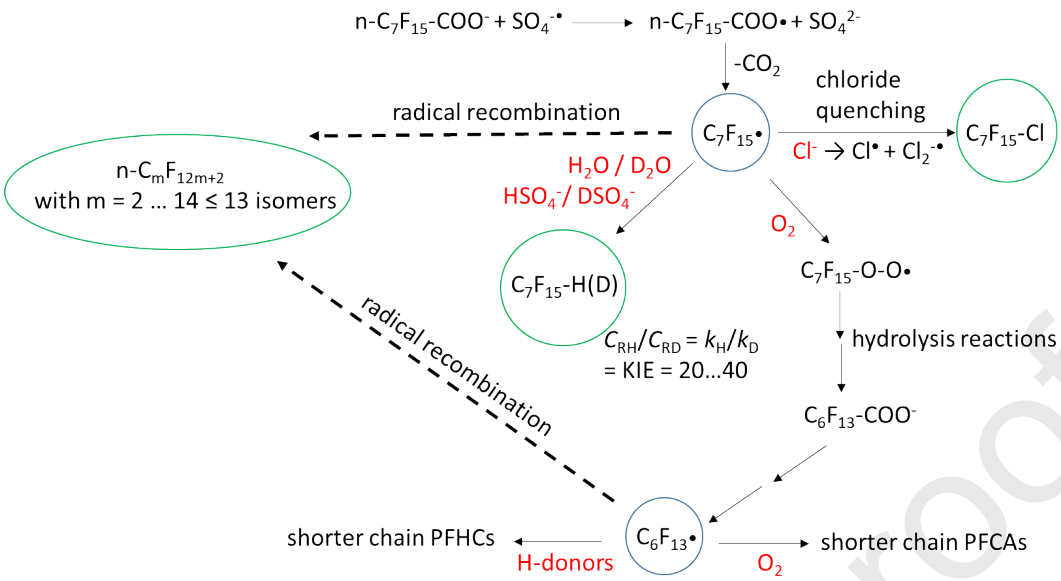
We hypothesize that PFOA accumulation on FeS particles is the key factor which enables its oxidation even if NOM or dissolved anions are present. Thereby, the higher local concentration in proximity to radical generation at the FeS surface causes a shift in relative reaction rates (Table 2). As a rather hydrophobic mineral compared to Fe^0 with its FeO_x surface coating [65], FeS is able to adsorb PFOA to a significant extent (with measured K_D values for PFOA of up to 500 L kg^{-1}, Figure 1), which is enhanced due to the matrix components (see Figure S4). This keeps considerable

proportions of PFOA within the range of influence of the short-lived radicals generated on FeS, whereas the competitors, which are dissolved in the water phase, are largely outside this range. This could be a reason for the lower vulnerability of the PFOA oxidation to quenching ions, and for the advantage of FeS-activated PS over that activated in homogenous solution (see Figure S8). In summary, the reaction of PFOA with FeS-activated PS still proceeds in the presence of various common radical quenchers, including chloride at concentrations as high as 100 mM.

3.4 Fate of perfluoroalkyl radicals in FeS-activated suspensions vs. homogeneous solutions

In order to elucidate the reaction mechanism of FeS-assisted degradation of perfluorinated carboxylic acids (PFCAs), we investigated more deeply the fate of a key intermediate, the perfluoroalkyl radical (n-C_mF_{2m+1}•, see section 7 in the SI part). A number of reaction pathways are presented in Scheme 1. The preferred reaction is the recombination of n-C_mF_{2m+1}• with dissolved oxygen (O_2), which leads to the formation of shorter-chain PFCAs. In the absence of O_2, alternative reaction pathways such as radical recombination or H-abstraction, e.g. from the solvent water, are possible. The resulting products, perfluorinated alkanes and 1H-perfluoroalkanes, are highly volatile. They are detectable in the headspace phase above the aqueous phase, where they are protected against further radical attack.

Journal Pre-proofs



Scheme 1: Reaction pathways of perfluoroalkyl radicals from oxidation of PFOA in aqueous solution

The headspace analyses revealed significantly different product compositions, depending on the presence or absence of FeS. Briefly, in the inert gas phase (Ar) above homogeneous solutions, a cocktail of more than 18 perfluoroalkanes was identified (see Figure S9). Their yield was estimated as up to 25% of the converted PFOA. 1H-perfluoroalkanes were observed only as trace components (<0.1 mol-% of converted PFOA). Although linear perfluoroalkanes dominate, we also detected branched isomers. This indicates - unexpectedly - radical isomerization reactions on the level of the primary n-C_mF_{2m+1}• radicals. We did not detect any perfluoroalkenes, indicating that radical disproportionation reactions (2 C_mF_{2m+1}• → C_mF_{2m} + C_mF_{2m+2}) do not play a role.

The pattern of gaseous products in the presence of FeS as PS activator was dominated by the series of linear homologous 1H-perfluoroalkanes $C_mF_{2m+1}H$ with $m \leq 7$ (see Figure S10). When we consider extensive radical recombination as an indication of freely dissolved radicals, the opposite finding (lack of radical recombination products) points to surface-bound radicals with FeS. These radicals are not sufficiently mobile to find other surface radicals, but due to contact with the solvent molecules they can be stabilized by H-abstraction.

In some experiments we used an equimolar H_2O/D_2O mixture as solvent in order to trace the hydrogen abstraction by perfluoroalkyl radicals. From the molar ratios $C_mF_{2m+1}H/C_mF_{2m+1}D$ we determined kinetic isotope effects (KIE) k_H/k_D = 10 to 40, with k_H and k_D as rate constants for the abstraction of H and D, respectively, from available donors. Such high KIE values were also observed for H-abstraction by perfluoroalkyl radicals from a series of organic substrates in water and are in line with our present findings with water as H-donor molecule [66]. The KIE values determined in the present study are different for the two reaction systems (see Table S5 and Figure S11). For the primary n-C_7F_{15}-radical, they are about a factor of 2 lower in the FeS-mediated system, indicating different states of the precursor radicals, either attached to the surface of FeS (or at least surface-influenced) or freely dissolved in water. A detailed interpretation of the observed KIEs is further complicated by the overlay of at least two pairs of hydrogen donors under acidic conditions, i.e. H_2O/D_2O and HSO_4^-/DSO_4^-.

In further experiments, we added chloride (5 mM) as a potential radical quencher in order to interpret the results from section 3.3. Chloride can be oxidized by sulfate radicals to reactive radicals such as $Cl^\bullet$ and $Cl_2^{-\bullet}$ which are reaction partners for perfluoroalkyl radicals (n-$C_mF_{2m+1}^\bullet$ + $Cl_2^{-\bullet} \rightarrow$ n-$C_mF_{2m+1}Cl + Cl^-$). As expected, chloride inhibited the homogenous PFOA conversion and shifted the gaseous product composition to 1Cl-perfluoroalkanes (see Figure S12). We detected in all experiments in the presence of chloride the homologous series from 1-ClC_7F_{15} to 1-ClC_4F_9. The recombination between perfluoroalkyl radicals was largely suppressed in homogeneous solution, whereas the surface-attached radicals in the presence of FeS yielded a mixture of 1H- and 1Cl-perfluoroalkanes (about 30:70 mol/mol). This again underlines the different reactivities of perfluoroalkyl radicals as intermediates in the homogeneous vs. the heterogeneous reaction system, as well as the partial exclusion of radical quenchers from the surface-near reaction zone. In conclusion, these experiments show on the one hand that the fate of intermediates of PFOA

degradation depends on their speciation: either freely dissolved or surface-attached on FeS. On the other hand, it was shown that chloride has an influence on the reaction as well as on the degradation product pattern, as stated in section 3.3.

3.5 Influence of real groundwater and sediment on PFOA degradation

As shown in the previous sections, FeS particles are potent activators of PS and can support degradation of PFOA on the FeS surface, leading to an attenuation of radical quenchers. However, these experiments have so far only been carried out under artificial conditions. As a subsequent step, the degradation of PFOA in various water matrices (deionized water, tap water and a groundwater sample) and in the presence of sediment from a PFAS-contaminated site was investigated. The results in Figure 4 show that PFOA can be degraded in all of the water matrices tested. Highest reaction rates for PFOA removal were achieved in deionized water, but rate constants in tap- or groundwater are only slightly lower (Table 3). These results are in conformity with the results in section 3.3, showing only minor influence of various ions on the reaction when used in naturally occurring concentrations. PFOA degradation kinetics in tap- and groundwater are similar, despite the different ionic strengths and composition of the samples (see Table S1). Surprisingly, even the addition of sediment has no significant negative impact on the reaction rates (leaching results are summarized in Table S3), although it was suspected that the sediment would provide significant potential for radical quenching [67]. All of these findings agree with our assumption that the PFOA oxidation occurs mainly as a heterogeneous reaction at or near the FeS surface. This makes the degradation largely immune to sulfate radical quenchers, although these are inherently much more reactive.

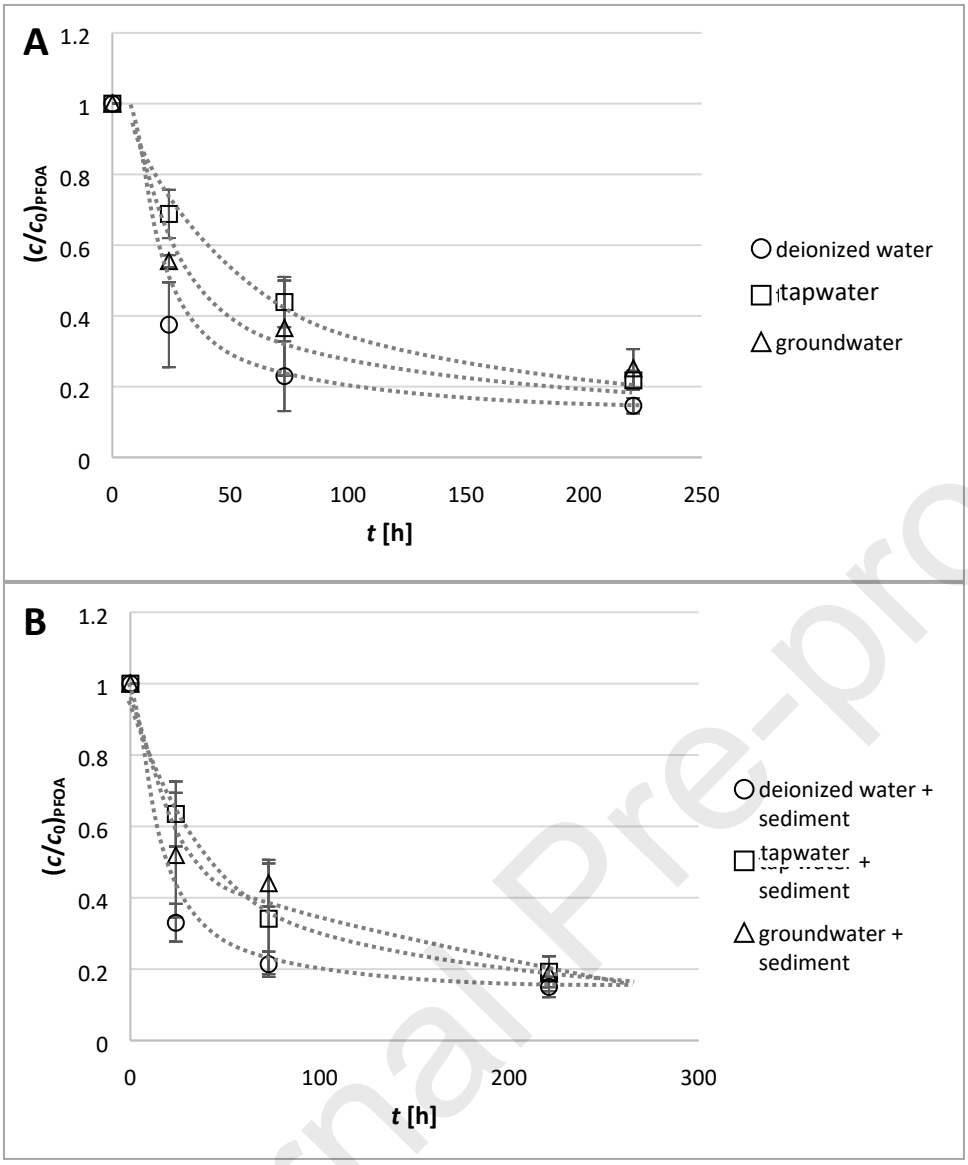


Figure 4: PFOA degradation by FeS-activated PS in various water matrices without (A) and with (B) site sediment ($c_{0,PFOA}$ = 10 mg L^{-1} = 2.4 · 10^{-2} mM, $c_{0,FeS}$ = 1 g L^{-1} = 11.4 mM, $c_{0,\,PS}$ = 30 g L^{-1} = 126 mM, $c_{sediment}$ = 100 g L^{-1}, pH_{start} = 7 and $pH_{final} \leq 2$). Error bars represent at least four individual experiments and show the mean deviation of single values from the mean value.

Journal Pre-proofs

Table 3: Observed first-order rate constants [in 10^{-2} h^{-1}] of PFOA degradation by FeS-activated PS in various water matrices in the first 100 hours. Experimental conditions as given in Fig. 4.

Deionized water	Tapwater	Groundwater	Deionized water + sediment	Tapwater + sediment	Groundwater + sediment
4.1 ± 0.7	1.2 ± 0.1	1.5 ± 0.1	4.6 ± 0.8	1.5 ± 0.1	1.9 ± 0.1

It can be seen in Figure 4 that after 220 h, about 20 % of the PFOA still remains under the various reaction conditions tested, even though PS was still present in the system. This implies a stagnation of the reaction, which was also found for PS activation with UV and microwave [21, 50, 51, 68] irradiation. In the present study, a plausible explanation for the stagnation is considered to be the increased dissolution of FeS with lower pH values and thus an increase in the quencher concentration c_{Fe2+}. As can be seen in Figure S14, the PS decomposition also stops, which results in a stagnation of PFOA degradation.

The results presented in this section show that degradation of PFOA by FeS-activated PS can be conducted even under near-natural conditions – in groundwater and after addition of sediment samples. This allows an optimistic performance forecast for field deployment of FeS particles as a new material for oxidation with sulfate radicals – and it provides an opportunity to develop a new cost-efficient degradation tool for perfluorinated carboxylic acids (compare chapter 9 in SI part).

4 Summary and conclusion

In the framework of this study, the application of FeS-activated persulfate for PFOA degradation was examined. Adjustment of the reagent ratios revealed highest efficiency at high concentrations of FeS as activator, PS as oxidant and PFOA as target contaminant. However, the reaction was also observed under significantly less favorable conditions. High PS concentrations deliver sufficient

oxidation power to overcome competing side-reactions and thus enable PFOA degradation, whilst higher FeS concentrations lead to higher production rates of sulfate radicals and thereby enhance productivity of the system.

Moving from pure to near-natural water matrices, the low reaction rate of PFOA with sulfate radicals requires competitor exclusion from the direct proximity of the reaction. Degradation of PFOA with sulfate radicals was enabled by considerable enrichment of PFOA at the FeS surface (K_D = 100 – 500 L kg^{-1} at a specific surface area of 0.9 m^2 g^{-1}), and thus spatial decoupling of the PFOA degradation from reaction of matrix components. This was proven by the low adverse effect of even high concentrations of competing reactants such as NOM (up to 100 mg L^{-1}), Cl^- and NO_3^- (up to 100 mM) as well as by the different PFOA product pattern in homogenous and heterogeneous reactions. The approach of enhancing PFOA's degradation rate by increasing its local concentration at the site of radical generation is promising.

Nevertheless, there is still room for further research related to the topic of activation of PS by FeS or other potent heterogeneous activators providing efficient PFOA adsorption. Some uncertainties were already brought up in this work, such as the slowdown of PFOA degradation during the reaction progress or the final clarification of gaps in the mass balance. Furthermore, open questions remain regarding the applicability to other groundwater pollutants or even other PFAS, such as shorter-chain perfluorinated carboxylic acids or fluorotelomer alcohols. Another urgent issue is the lack of approaches for the remediation of groundwater contaminated with perfluorinated sulfonic acids, for which the presented approach unfortunately fails.

However, significant PFOA degradation was achieved in batch experiments with real site waters and sediments, which open up an optimistic perspective for *in-situ* deployment of the presented remediation system. Therefore, the remediation approach discussed in this study represents a

valuable contribution to solving one of the most pressing problems for water treatment at the present time. Pilot-scale tests for evaluation of the field applicability of this technique are currently under study.

ASSOCIATED CONTENT

Supporting Information. Supplementary data and methodical comments associated with this article can be found in the online version, at …

Author Contributions

The manuscript was written with contributions of all authors. All authors have given approval to the final version of the manuscript.

The authors declare no competing financial interest.

ACKNOWLEDGEMENTS

This work was supported by funds of the German Federal Ministry of Education and Research (BMBF) in the frame of the project CONTASORB [grant number 03XP0090A] and partially also by Fraunhofer Cluster of Excellence Integrated Energy Systems CINES.

References

1. Giesy, J.P. and K. Kannan, *Global distribution of perfluorooctane sulfonate in wildlife.* Environmental Science & Technology, 2001. **35**(7): p. 1339-1342.
2. Kucharzyk, K.H., et al., *Novel treatment technologies for PFAS compounds: A critical review.* Journal of Environmental Management, 2017. **204**: p. 757-764.

Journal Pre-proofs

3. Trojanowicz, M., et al., *Advanced oxidation/reduction processes treatment for aqueous perfluorooctanoate (PFOA) and perfluorooctanesulfonate (PFOS) – A review of recent advances.* Chemical Engineering Journal, 2018. **336**: p. 170-199.

4. Liu, W., et al., *A review on perfluoroalkyl acids studies: Environmental behaviors, toxic effects, and ecological and health risks.* Ecosystem Health and Sustainability, 2019. **5**(1): p. 1-19.

5. Nzeribe, B.N., et al., *Physico-chemical processes for the treatment of per- and polyfluoroalkyl substances (PFAS): A review.* Critical Reviews in Environmental Science and Technology, 2019. **49**(10): p. 866-915.

6. Mudumbi, J.B.N., et al., *Recent developments in polyfluoroalkyl compounds research: a focus on human/environmental health impact, suggested substitutes and removal strategies.* Environmental Monitoring and Assessment, 2017. **189**(8): p. 402.

7. Xiao, F., *Emerging poly- and perfluoroalkyl substances in the aquatic environment: A review of current literature.* Water Research, 2017. **124**: p. 482-495.

8. Banzhaf, S., et al., *A review of contamination of surface-, ground-, and drinking water in Sweden by perfluoroalkyl and polyfluoroalkyl substances (PFASs).* Ambio, 2017. **46**(3): p. 335-346.

Journal Pre-proofs

9. Hekster, F.M., R.W.P.M. Laane, and P. de Voogt, *Environmental and toxicity effects of perfluoroalkylated substances*, in *Reviews of environmental contamination and toxicology*, P.d. Voogt, Editor. 2003, Springer New York: New York, NY. p. 99-121.

10. Lau, C., et al., *Perfluoroalkyl acids: A review of monitoring and toxicological findings.* Toxicological Sciences, 2007. **99**(2): p. 366-394.

11. Fang, C., M. Megharaj, and R. Naidu, *Electrochemical advanced oxidation processes (EAOP) to degrade per- and polyfluoroalkyl substances (PFASs)*, in *Journal of Advanced Oxidation Technologies*. 2017.

12. Cheng, J., et al., *Sonochemical degradation of perfluorooctane sulfonate (PFOS) and perfluorooctanoate (PFOA) in groundwater: Kinetic effects of matrix inorganics.* Environmental science & technology, 2009. **44**: p. 445-50.

13. Schaefer, C., et al., *Electrochemical treatment of perfluorooctanoic acid (PFOA) and perfluorooctane sulfonic acid (PFOS) in groundwater impacted by aqueous film forming foams (AFFFs).* Journal of Hazardous Materials, 2015. **295**(15): p. 170-175.

14. Carter, K. and J. Farrell, *Oxidative destruction of perfluorooctane sulfonate using boron-doped diamond film electrodes.* Environmental science & technology, 2008. **42**: p. 6111-5.

Journal Pre-proofs

15. Chen, J. and P. Zhang, *Photodegradation of perfluorooctanoic acid in water under irradiation of 254 nm and 185 nm light by use of persulfate.* Water Science and Technology, 2006. **54**(11-12): p. 317-325.

16. Song, C., et al., *Photodegradation of perfluorooctanoic acid by synthesized TiO2–MWCNT composites under 365nm UV irradiation.* Chemosphere, 2012. **86**(8): p. 853-859.

17. Kishimoto, N. and K. Doda, *Effects of pH and coexisting chemicals on photolysis of perfluorooctane sulfonate using an excited xenon dimer lamp.* Water Science and Technology, 2017. **77**(1): p. 108-113.

18. Qian, L., et al., *Degradation of perfluorooctanoic acid adsorbed on Fe-zeolites with molecular oxygen as oxidant under UV-A irradiation.* Applied Catalysis B: Environmental, 2020. **278**: p. 119283.

19. Qian, L., F.-D. Kopinke, and A. Georgi, *Photodegradation of Perfluorooctanesulfonic Acid on Fe-Zeolites in Water.* Environmental Science & Technology, 2021. **55**(1): p. 614-622.

20. Qian, Y., et al., *Perfluorooctanoic acid degradation using UV–persulfate process: modeling of the degradation and chlorate formation.* Environmental Science & Technology, 2016. **50**(2): p. 772-781.

21. Lutze, H.V., et al., *Degradation of perfluorinated compounds by sulfate radicals – New mechanistic aspects and economical considerations.* Water Research, 2018. **129**: p. 509-519.

22. Hori, H., et al., *Efficient decomposition of environmentally persistent perfluorooctanesulfonate and related fluorochemicals using zerovalent iron in subcritical water.* Environmental science & technology, 2006. **40**(3): p. 1049-54.

23. Yang, S., et al., *Defluorination of aqueous perfluorooctanesulfonate by activated persulfate oxidation.* PLOS ONE, 2013. **8**(10): p. e74877.

24. Luo, S., et al., *Mechanistic insight into reactivity of sulfate radical with aromatic contaminants through single-electron transfer pathway.* Chemical Engineering Journal, 2017. **327**: p. 1056-1065.

25. Vecitis, C.D., et al., *Treatment technologies for aqueous perfluorooctanesulfonate (PFOS) and perfluorooctanoate (PFOA).* Frontiers of Environmental Science & Engineering in China, 2009. **3**(2): p. 129-151.

26. Park, S., et al., *Heat-activated persulfate oxidation of PFOA, 6:2 fluorotelomer sulfonate, and PFOS under conditions suitable for in-situ groundwater remediation.* Chemosphere, 2016. **145**: p. 376-383.

27. Houtz, E.F. and D.L. Sedlak, *Oxidative conversion as a means of detecting precursors to perfluoroalkyl acids in urban runoff.* Environmental Science & Technology, 2012. **46**(17): p. 9342-9349.

28. Anipsitakis, G.P. and D.D. Dionysiou, *Degradation of organic contaminants in water with sulfate radicals generated by the conjunction of*

Journal Pre-proofs

peroxymonosulfate with cobalt. Environmental Science & Technology, 2003. **37**(20): p. 4790-4797.

29. Matzek, L.W. and K.E. Carter, *Activated persulfate for organic chemical degradation: A review.* Chemosphere, 2016. **151**(Supplement C): p. 178-188.
30. Waldemer, R.H., et al., *Oxidation of chlorinated ethenes by heat-activated persulfate: Kinetics and products.* Environmental Science & Technology, 2007. **41**(3): p. 1010-1015.
31. Johnson, R.L., P.G. Tratnyek, and R.O.B. Johnson, *Persulfate persistence under thermal activation conditions.* Environmental Science & Technology, 2008. **42**(24): p. 9350-9356.
32. Guan, Y.-H., et al., *Influence of pH on the formation of sulfate and hydroxyl radicals in the UV/peroxymonosulfate system.* Environmental Science & Technology, 2011. **45**(21): p. 9308-9314.
33. Anipsitakis, G.P. and D.D. Dionysiou, *Radical generation by the interaction of transition metals with common oxidants.* Environmental Science & Technology, 2004. **38**(13): p. 3705-3712.
34. Yuan, Y., et al., *Degradation of p-chloroaniline by persulfate activated with ferrous sulfide ore particles.* Chemical Engineering Journal, 2015. **268**(Supplement C): p. 38-46.

Journal Pre-proofs

35. Neta, P., R.E. Huie, and A.B. Ross, *Rate constants for reactions of inorganic radicals in aqueous-solution.* Journal of Physical and Chemical Reference Data, 1988. **17**(3): p. 1027-1284.

36. Oh, S.-Y., et al., *Degradation of 2,4-dinitrotoluene by persulfate activated with iron sulfides.* Chemical Engineering Journal, 2011. **172**(2): p. 641-646.

37. Fan, J., et al., *Mackinawite (FeS) activation of persulfate for the degradation of p-chloroaniline: surface reaction mechanism and sulfur-mediated cycling of iron species.* Chemical Engineering Journal, 2018. **333**: p. 657-664.

38. Chen, H., et al., *Degradation of 2,4-dichlorophenoxyacetic acid in water by persulfate activated with FeS (Mackinawite).* Chemical Engineering Journal, 2017. **313**: p. 498-507.

39. He, J., et al., *Magnetic ball-milled FeS@biochar as persulfate activator for degradation of tetracycline.* Chemical Engineering Journal, 2021. **404**: p. 126997.

40. Sühnholz, S., F.-D. Kopinke, and K. Mackenzie, *Reagent or catalyst? – FeS as activator for persulfate in water.* Chemical Engineering Journal, 2020. **387**: p. 123804.

41. Kutsuna, S. and H. Hori, *Rate constants for aqueous-phase reactions of SO_4^- with $C_2F_5C(O)O^-$ and $C_3F_7C(O)O^-$ at 298 K.* International Journal of Chemical Kinetics, 2007. **39**(5): p. 276-288.

42. Maruthamuthu, P., S. Padmaja, and R.E. Huie, *Rate constants for some reactions of free radicals with haloacetates in aqueous solution.* International Journal of Chemical Kinetics, 1995. **27**(6): p. 605-612.

43. Padmaja, S., P. Neta, and R.E. Huie, *Rate constants for some reactions of inorganic radicals with inorganic ions. Temperature and solvent dependence.* International Journal of Chemical Kinetics, 1993. **25**(6): p. 445-455.

44. Driver, S.J. and E.M. Perdue, *Acidic functional groups of suwannee river natural organic matter, humic acids, and fulvic acids*, in *Advances in the physicochemical characterization of dissolved organic matter: Impact on natural and engineered systems*, F. Rosario-Ortiz, Editor. 2014, American Chemical Society. p. 75-86.

45. Reschetilowski, W., *Grundlagen der heterogenen Katalyse*, in *Einführung in die Heterogene Katalyse*. 2015, Springer Berlin Heidelberg: Berlin, Heidelberg. p. 47-66.

46. Zhao, L., et al., *Comparison of the sorption behaviors and mechanisms of perfluorosulfonates and perfluorocarboxylic acids on three kinds of clay minerals.* Chemosphere, 2014. **114**: p. 51-58.

47. Bebie, J., et al., *Surface charge development on transition metal sulfides: An electrokinetic study.* Geochimica et Cosmochimica Acta, 1998. **62**(4): p. 633-642.

48. Van den Bergh, M., et al., *Highly Selective Removal of Perfluorinated Contaminants by Adsorption on All-Silica Zeolite Beta.* Angewandte Chemie International Edition, 2020. **59**(33): p. 14086-14090.

49. Bruton, T.A. and D.L. Sedlak, *Treatment of perfluoroalkyl acids by heat-activated persulfate under conditions representative of in situ chemical oxidation.* Chemosphere, 2018. **206**: p. 457-464.

50. Yin, P., et al., *Activated persulfate oxidation of perfluorooctanoic acid (PFOA) in groundwater under acidic conditions.* International journal of environmental research and public health, 2016. **13**(6): p. 602.

51. Lee, Y., et al., *Decomposition of perfluorooctanoic acid by microwaveactivated persulfate: Effects of temperature, pH, and chloride ions.* Frontiers of Environmental Science & Engineering, 2012. **6**(1): p. 17-25.

52. Bao, Z.-C. and J.R. Barker, *Temperature and ionic strength effects on some reactions involving sulfate radical [$SO_4^-(aq)$].* The Journal of Physical Chemistry, 1996. **100**(23): p. 9780-9787.

53. Monk, D.J., D.S. Soane, and R.T. Howe, *A review of the chemical reaction mechanism and kinetics for hydrofluoric acid etching of silicon dioxide for surface micromachining applications.* Thin Solid Films, 1993. **232**(1): p. 1-12.

Journal Pre-proofs

54. Vithanage, M., et al., *Modeling sorption of fluoride on to iron rich laterite.* Colloids and Surfaces A: Physicochemical and Engineering Aspects, 2012. **398**: p. 69-75.

55. Reynolds, D.S. and K.D. Jacob, *Method for determination of fluorine in phosphate rock and phosphatic slags.* Industrial & Engineering Chemistry Analytical Edition, 1931. **3**(4): p. 366-370.

56. Heerah, K., et al., *Benchtop 19F NMR spectroscopy as a practical tool for testing of remedial technologies for the degradation of perfluorooctanoic acid, a persistent organic pollutant.* Magnetic Resonance in Chemistry, 2020. **58**(12): p. 1160-1167.

57. Costanza, J., et al., *PCE oxidation by sodium persulfate in the presence of solids.* Environmental Science & Technology, 2010. **44**(24): p. 9445-9450.

58. Gu, X., et al., *Oxidation of 1,1,1-trichloroethane stimulated by thermally activated persulfate.* Industrial & Engineering Chemistry Research, 2011. **50**(19): p. 11029-11036.

59. Ghosh, K. and M. Schnitzer, *Macromolecular structures of humic subtances* Soil Science, 1980. **129**(5): p. 266-276.

60. Huie, R.E. and C.L. Clifton, *Temperature dependence of the rate constants for reactions of the sulfate radical, SO_4^-, with anions.* The Journal of Physical Chemistry, 1990. **94**(23): p. 8561-8567.

61. Herrmann, H., A. Reese, and R. Zellner, *Time-resolved UV/VIS diode array absorption spectroscopy of SO_x^-(x=3, 4, 5) radical anions in aqueous solution.* Journal of Molecular Structure, 1995. **348**: p. 183-186.

62. Løgager, T., K. Sehested, and J. Holcman, *Rate constants of the equilibrium reactions $SO_4^{\cdot-} + HNO_3 \rightleftarrows HSO_4^- + NO_3^{\cdot}$ and $SO_4^{\cdot-} + NO_3^- \rightleftarrows SO_4^{2-} + NO_3^{\cdot}$.* Radiation Physics and Chemistry, 1993. **41**(3): p. 539-543.

63. Lutze, H.V., et al., *Degradation of Chlorotriazine Pesticides by Sulfate Radicals and the Influence of Organic Matter.* Environmental Science & Technology, 2015. **49**(3): p. 1673-1680.

64. Wacławek, S., et al., *Chemistry of persulfates in water and wastewater treatment: A review.* Chemical Engineering Journal, 2017. **330**: p. 44-62.

65. Xu, J., et al., *Reactivity, Selectivity, and Long-Term Performance of Sulfidized Nanoscale Zerovalent Iron with Different Properties.* Environmental Science & Technology, 2019. **53**(10): p. 5936-5945.

66. Cradlebaugh, J.A., et al., *Large primary kinetic isotope effects in the abstraction of hydrogen from organic compounds by a fluorinated radical in water.* Organic & Biomolecular Chemistry, 2004. **2**(14): p. 2087-2091.

67. Crincoli, K.R., C. Green, and S.G. Huling, *Sulfate radical scavenging by mineral surfaces in persulfate-driven oxidation systems: Reaction rate constants and implications.* Environmental Science & Technology, 2020. **54**(3): p. 1955-1962.

68. Hamid, H. and L.Y. Li, *Fate of perfluorooctanoic acid (PFOA) in sewage sludge during microwave-assisted persulfate oxidation treatment.* Environmental Science and Pollution Research, 2018. **25**(10): p. 10126-10134.

Declaration of interests

☒ The authors declare that they have no known competing financial interests or personal relationships that could have appeared to influence the work reported in this paper.

☐The authors declare the following financial interests/personal relationships which may be considered as potential competing interests:

Highlights:

- FeS/peroxydisulfate system degrades PFOA in water under various conditions

Journal Pre-proofs

- Surface enrichment helps to degrade PFOA even under unfavorable bulk conditions
- Heterogeneous PFOA degradation occurs in presence of high chloride concentrations
- PFOA was successfully degraded in real site water and sediment suspensions
- FeS/peroxydisulfate system proposed as tool for *in-situ* degradation of PFOA

Journal Pre-proofs